Electron induced dissociation in the condensed-phase nitromethane: II. Desorption of neutral fragments

2010 J. Phys.: Condens. Matter 22 084003

(http://iopscience.iop.org/0953-8984/22/8/084003)

IOP Publishing Journal of Physics: Condensed Matter

J. Phys.: Condens. Matter **22** (2010) 084003 (9pp) doi:10.1088/0953-8984/22/8/084003

Electron induced dissociation in the condensed-phase nitromethane: II. Desorption of neutral fragments

M Bazin[1], S Ptasinska[1,2], A D Bass[1,4], L Sanche[1,2], E Burean[3] and P Swiderek[3]

[1] Département de Médecine Nucléaire et Radiobiologie, Faculté de Médecine, Université de Sherbrooke, Sherbrooke, QC, J1H 5N4, Canada
[2] Department of Physics and Astronomy, The Open University, Walton Hall, Milton Keynes, MK7 6AA, UK
[3] Institut für Angewandte und Physikalische Chemie, Universität Bremen, Leobener Straße/NW2, Postfach 330440, 28334 Bremen, Germany

E-mail: Andrew.Bass@USherbrooke.ca

Received 1 July 2009, in final form 18 August 2009
Published 4 February 2010
Online at stacks.iop.org/JPhysCM/22/084003

Abstract

Low energy electron induced dissociation in multilayer films of nitromethane (CD_3NO_2) was investigated by high resolution electron energy loss spectroscopy (HREELS) and by the electron stimulated desorption (ESD) of neutral species. HREELS measurements show that the lowest electronic states of the condensed molecule are very similar to those seen in the gas phase. Desorbed neutrals were detected using combined non-resonant multi-photon ionization at 355 nm and time of flight mass spectrometry. The most intense signals detected were those of CD_3^+ and NO^+ and are attributed primarily to the desorption of CD_3 and NO_2 fragments following molecular dissociation via low-lying electronic excited states of nitromethane (the detected NO^+ being the result of the dissociative ionization of NO_2). By varying the time delay between the incident electron pulse and the ionizing laser pulse, it is possible to measure the kinetic energy distributions of desorbing fragments. The kinetic energy distributions above ~5 eV appear invariant with incident electron energy, indicating that the same desorption process (dissociation via low-lying electronic states) operates at all the studied incident energies. Nevertheless, measurements of neutral yields as functions of incident electron energy demonstrate that excitation of the dissociative electronic states also proceeds via previously identified transient negative ions. At energies less than ~5 eV, contributions from dissociative electron attachment are also observed in the yield of CD_3 and other neutral fragments.

(Some figures in this article are in colour only in the electronic version)

1. Introduction

Nitromethane (NM) is the simplest nitroalkane molecule and is used widely both as a solvent and reagent in organic synthesis. It has found application as an additive in high performance engine fuels (less oxygen being required to completely oxidize NM than for hydrocarbons) and is known as a monopropellant and explosive. The comparative simplicity of the molecule has meant that NM has been used as a prototypical explosive in theoretical models of detonation [1–3]. The explosive properties of NM are clearly linked to its molecular structure and it is, at least in part, for this reason that the molecule has been the subject of numerous studies into its dissociation, whether induced by photons e.g., [4–9] or electrons, e.g., [10–14].

Most of these experimental studies into molecular dissociation have concerned the isolated molecule despite the fact that explosive detonation is only possible in the liquid phase; exceptions include recent results by Guo *et al* [9] and

[4] Author to whom any correspondence should be addressed.

earlier work by Blais *et al* [15]. In our earlier paper [16], we investigated, for condensed nitromethane, dissociative processes leading to the production of charged fragments using the technique of electron stimulated desorption (ESD) at incident electron energies between 0 and 20 eV. Anion yield functions demonstrated the role of transient negative ions (TNI), dissociative electron attachment (DEA) and dipolar dissociation (DD) in the production of negatively charged fragments at these lower energies, as is common for many studied molecular solids [17]. Evidence for ion–molecule reactions was also obtained, as well as the energetic thresholds for the production of cationic fragments. In this paper we present data concerning the production of neutral fragment species from electron bombarded films of deuterated nitromethane (d_3-NM). Since for gas-phase NM, molecular dissociation via excited states is important, we have also used high resolution electron energy loss spectroscopy (HREELS) to observe the lowest electronic states of the condensed molecule.

In section 2, we briefly review the literature concerning the electron stimulated desorption of neutral species. In section 3, the novel experimental methods employed in this study are described, and section 4 focuses on our experimental results, first reporting on the electronic spectroscopy of d_3-NM films under electron impact and then our observations of neutral particle desorption. In both cases, measurements are compared to data obtained in gas-phase experiments as we attempt to identify the mechanisms responsible for the observed electron stimulated desorption.

2. Electron stimulated desorption of neutrals from thin films

The electron stimulated desorption of *neutral species* from *physisorbed molecular solids* is a subject that has received comparatively little attention, when compared to that devoted to the desorption of charged particles from similar targets. Nevertheless neutral species represent the majority of particles desorbed (or sputtered) when ionizing radiation is incident on thin films and solids [18]. The comparative scarcity of information on this subject reflects both the difficulties inherent in measuring the desorption of neutral species and the number and complexity of desorption mechanisms.

A priori neutral species can be desorbed from electron irradiated films via a number of different processes. In our previous paper [16] we observed that DEA is effective in desorbing various anions from the multilayer (and sub-monolayer on Kr) films of NM and d_3-NM. When DEA occurs and desorbs anions, it is also likely that the neutral fragments created simultaneously by this process, will similarly desorb. Indeed in earlier work, several of the present authors have linked structures seen in the yield functions of neutral species, desorbed in metastable states, with DEA resonances seen in anion yield functions from films of CO_2 [19] and N_2O [20]. A report by Lane and Orlando [21] shows that DEA is an important mechanism for the desorption of neutral fragment species from multilayer films of $SiCl_4$ irradiated with low energy electrons (LEE). Likewise neutral fragments generated via other molecular dissociation processes, for example the excitation of specific dissociative electronic states, whether directly or indirectly (e.g., via a TNI), should be expected to contribute to the desorbed yield of neutrals. Indeed, such mechanisms have been invoked in describing the yield functions of specific neutral fragments desorbed from electron irradiated amorphous solid water [22] and from self-assembled monolayers (SAMs) of short oligonucleotides chemisorbed on gold substrates [23, 24].

In addition to molecular dissociation, experiments on *chemisorbed* systems have provided examples of other mechanisms by which neutral species, either fragments or intact molecules are produced [18]. From a semi-classical point of view and at incident energies relevant to the present work, two broad classes of desorption mechanisms are relevant. In the *Menzel–Gomer–Redhead (MGR)* model [25, 26] of desorption induced by electronic transitions (DIET), an adsorbate complex is electronically excited onto a *repulsive* potential energy (PE) surface (ionic or neutral) of some bonding mode of the adsorbate (either with respect to the substrate, or within the molecule). By relaxing along this PE surface and moving *away from the substrate*, the adsorbate (or some part of it) can gain sufficient kinetic energy to desorb, even if, as is usually the case, the initial excitation is quenched by charge or energy transfer with the substrate. In contrast, in the *Antoniewicz model* [27] (arguably, an extension of the MGR picture), the adsorbate–substrate is first excited onto an *attractive* potential, so that the adsorbate (or some part of it) begins to *move towards the surface*. When the excitation is quenched, the system returns to the ground state (or another state of lower energy) at a point on the repulsive part of the lower state's PE surface. Consequently the adsorbate (or some part of it) begins to move *away* from the substrate and will desorb provided that sufficient kinetic energy (KE) has been gained during relaxation along the *two* PE surfaces.

As already noted, information on the ESD of neutral species from *physisorbed* solids, particularly molecular solids, is somewhat limited. The electron stimulated desorption of neutrals (in ground and excited states) has been reported for LEE irradiated rare gas solids (RGS) [28]. In these materials desorption proceeds via self-trapping of excitons either as an atomic center (atomic self-trapped exciton or a-STE) at the film vacuum interface or as a molecular center within the solid. In solids such as Ar and Ne possessing a positive V_0 (i.e., the conduction band lies above the vacuum level) the a-STE experiences a net repulsive interaction with neighboring atoms sufficient to desorb the excited atom. This ejection process, termed the '*cavity ejection mechanism*' [29] is thus mediated by a purely repulsive potential and may be considered a special case of the MGR desorption model. The cavity ejection mechanism is also responsible for the desorption of excited N_2 molecules from solid N_2 [30]. In contrast, the molecular-self-trapped exciton (m-STE) occurring in RGS can be pictured as an excited dimer embedded within the lattice [28]. Decay by UV-photon emission returns the dimer to its electronic ground state but at an inter-nuclear separation much smaller than that for equilibrium. Subsequent relaxation thus provides sufficient KE to desorb a ground state atom and the desorption process is

thus reminiscent of the model proposed by Antoniewicz [27]. In fact, the KE released may be sufficient to desorb several neighboring atoms through collision cascades [31].

Using an electron impact ionization technique, Feulner *et al* [32] have studied the energetic thresholds for the ESD of neutrals from a number of physisorbed solids (i.e., N_2, CO, O_2 and NO). For the materials studied, it was concluded that desorption mechanisms based on molecular fragmentation were relatively unimportant. Instead it was observed that even low-lying triplet excitations could effectively stimulate desorption of intact molecules, that the desorption cross sections were roughly proportional to those of net electronic excitation, and that direct vibrational excitation (up to $\nu = 8$) was not efficient in initiating desorption. The authors suggested desorption in these molecular solids might be dominated by radiationless conversion of electronic levels into very high vibrational levels e.g., ($\nu > 20$).

3. Experimental details

Energy loss measurements were performed in Bremen using a conventional HREEL spectrometer with cylindrical deflectors [33] incorporated in an ion-pumped UHV system reaching a base pressure in the 10^{-11} Torr range. The setup has been described in detail previously [34]. The combined resolution of the two energy selectors was set between 13 and 15 meV full width at half maximum of the elastic peak. A current of the order of 0.1 nA, as measured with a picoamperemeter, was applied to the platinum substrate. The incident electron energy (E_i) was calibrated within ± 0.2 eV as described previously [34].

Nitromethane for the Bremen experiments was purchased from Merck–Schuchardt at a stated purity of 98% and used as received. Thin molecular films were initially prepared from the gas phase using a gas-handling manifold. Known quantities of gas, measured by the differential pressure drop in a calibrated volume, were leaked into the vacuum chamber via a stainless steel capillary having an opening located just in front of a polycrystalline platinum substrate that was cooled by a closed-cycle He cryostat. For these experiments, the substrate was held at 60 K to prevent contamination with residual gases like CO. It must be noted that this heating of the substrate raised the chamber pressure into the high 10^{-10} Torr range causing a rise in background noise due to electrons from the ion pump. The thickness of the condensed NM films was estimated at 3–7 molecular layers from the amount of gas needed to deposit a monolayer, assuming no change in sticking coefficient for the adlayers. The amount of gas required for the formation of a monolayer was simply deduced from a comparison with measurements on other molecules of similar size [35, 36].

Desorption measurements were performed in Sherbrooke. A description of the ESD instrument and its use for measuring the desorption of charged particles from thin molecular solids has already been given [16]. In brief, experiments are performed under UHV conditions, where films of d_3-NM (99% atomic purity) are grown on a Pt foil substrate (held at temperature 'T', variable between 15 and 300 K), and exposed to low energy electrons produced by an electron gun (Kimball Physics ELG-2) set at an incidence angle of 45° with respect to the substrate normal. The gun is operated in a pulsed mode, which delivers a current of $\sim 10^{-6}$ A within time-periods of 0.05–1 μs duration. The absolute electron energy scale of the incident beam is calibrated by taking 0 eV as the onset of current transmission to the platinum film, with an estimated error of about ± 0.5 eV

Mass spectrometry of desorbed species (ions and neutrals) is achieved by means of time of flight (ToF) analysis using a reflectron time of flight mass analyzer (Kore Technology R-500) positioned along the surface normal, at 10 mm from the sample. *Desorbed neutrals* are detected by focusing the pulsed output of a frequency tripled Nd:YAG laser (Spectra Physics Lab 170) to a point ~ 0.5 mm in front of the Pt foil. The laser light has a wavelength of 355 nm and is delivered in a pulse of ~ 5 ns duration and energy 50–70 mJ at repetition rate of 50 Hz. By timing the arrival of the laser pulse, neutral species desorbed during an electron pulse can be ionized by a non-resonant multi-photon ionization (MPI) process. Ions created in this manner, can be injected in the mass analyzer by applying a positive voltage to the Pt substrate. (+2 kV, rise-time 30 ns, pulse width of 2 μs.) While the MPI process induces significant molecular fragmentation, it is possible by controlling the time delay between electron and photon pulses to study the KE of desorbed neutrals. The cationic fragments of desorbed neutral species are easily differentiated from the desorbed cations by recording spectra with and without application of the laser pulse. Cation yields per electron pulse, are typically 2–3 orders of magnitude lower than the detected neutral signal.

By recording mass spectra at different incident electron energies it is possible to investigate the variation of anion signal with incident electron energy and so obtain a *yield function* for each anionic fragment. The statistical accuracy of these yield functions can be optimized by integrating the ion signal over the width of each mass peak.

It should be noted that in practice desorbed neutrals are difficult to detect, unless they are desorbed in suitably energetic states that decay by observable photon emission [37], or in the case of those neutrals desorbed in long-lived 'metastable' states, undergo non-radiative decay at the surface of a particle detector (e.g. a microchannel plate) [38]. Otherwise, detection requires that a desorbed neutral be ionized, which then allows the efficient collection and transport of such species using conventional ion-optics and additionally permits mass analysis. Desorbed neutral species may be ionized in vacua by a variety of means including electron and photon bombardment. Previously, resonant enhanced multi-photon ionization (REMPI) [39] schemes have demonstrated both high sensitivity and selectivity [40] (allowing for example, detection of specific ro-vibrational levels). Unfortunately this selectively also limits the usefulness of REMPI in cases where the identities of desorbed species are not already known. In contrast, ionization with a single high energy UV-photon (from a laser or synchrotron source) is much less selective but allows the simultaneous ionization of numerous different desorbed species [41]. Non-selectivity is also a property of the non-resonant multi-photon ionization scheme used in the

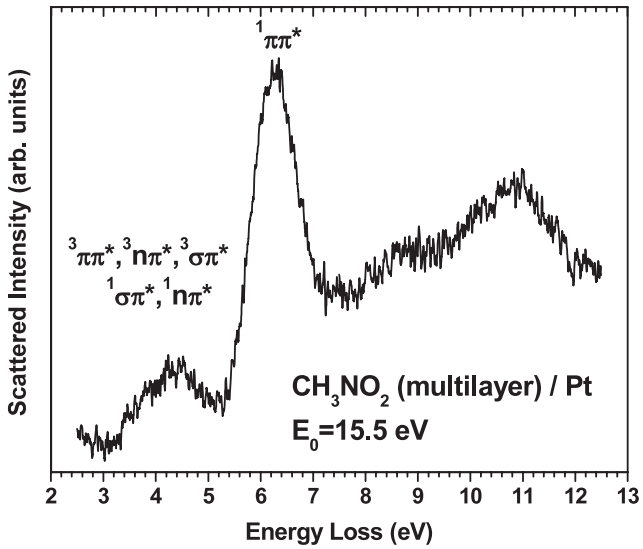

Figure 1. High resolution electron energy loss spectrum obtained with an incident electron energy of 15.5 eV ($E_i = 15.5$ eV) of multilayer CH_3NO_2 on Pt at 60 K.

present experiments. Unfortunately, the nanosecond timescale UV pulses used in the present work result in considerable molecular fragmentation via two competing routes [42, 43]; dissociative ionization or '*ladder switching*', where the molecule is dissociated first and neutral fragments are ionized by subsequent photons, and ionization followed dissociation, termed '*ladder climbing*', where the intact molecule is first ionized (by multi-photon absorption) then dissociates. In both cases such fragmentation complicates the interpretation of the mass spectra even if some useful information can be inferred using the technique [44].

4. Results and discussion

4.1. Electronic spectroscopy of nitromethane

Figure 1 shows the electron energy loss spectrum for a multilayer film of d_3-NM (3–7 ML) recorded at an incident electron energy of 15.5 eV and an electron current of 0.1 nA. The data of figure 1 is a composite of two smoothed spectra; one recorded for energy losses between 2.5 and 7.5 eV and the other for the range 7.5–12.5 eV. Background signals resulting from the elevated pressure varied between the two recordings and thus have been subtracted arbitrarily to fit the two spectra together. The vertical scale was normalized to the same recording time in each case.

The HREELS spectrum of figure 1, at least below ~8 eV, is remarkably similar to that obtained in the gas-phase HREELS experiments of Flicker *et al* [45], whose nomenclature will thus be employed in the following discussion. Below ~8 eV, the spectrum (figure 1) is characterized by two broad bands; a region of weak energy loss, between 3 and 5.4 eV and a much stronger energy loss feature between 5.4 and 7.5, with a maximum at 6.27 eV. Broadly similar features are observed in UV absorption measurements [12]. The lower energy loss manifold can be linked to several different excitations, in particular, the dipole allowed $^1B_1$ state ($\sigma \rightarrow \pi^*$) at 4.45 eV is thought to dominate, though contributions from at least one spin-allowed by dipole forbidden $n \rightarrow \pi^*$ transition is likely [45]. Both the present results, and the HREELS spectra of Flicker *et al* [45], exhibit a lower energy threshold for electronic excitation than is observed in optical spectroscopy. It has been suggested that an excited triplet state involving either a $\pi \rightarrow \pi^*$, $\sigma \rightarrow \pi^*$ or $n \rightarrow \pi^*$ transition and centered at 3.8 eV, is present in the electron impact data. Surprisingly, this latter state was not observed in trapped electron spectroscopy measurements [12].

The higher energy feature, observed at 6.25 eV in gas-phase VUV measurements is associated with an optically allowed $\pi \rightarrow \pi^*$ transition and consequent excitation of the $^1B_2$ state. At higher energies in the gas phase, various states have been observed at 8.3, 9.43 and 10.35 eV [45]. It is possible that some or all of these states may contribute to the spectrum of figure 1 although the statistics of the present data are insufficient to satisfactorily resolve these energy loss processes.

In the gas phase, excitation of states in either of the two lowest bands may lead to molecular dissociation and in both cases the dominant dissociation pathway involves cleavage to produce a methyl radical and nitrogen dioxide [4], i.e,

$$CH_3NO_2 + h\nu \rightarrow CH_3 + NO_2. \quad (1)$$

Blais [5] measured the C–N dissociation cross section at 193 nm as 1.7×10^{-17} cm^2 with a near unity quantum efficiency. Later experimental work [6–8] has indicated that at 193 nm there are two dissociation pathways; the major channel produced NO_2 in the first excited state ($\tilde{A}^2B_2$), with some (>10%) of this NO_2 containing sufficient internal energy for unimolecular dissociation to NO and O. A minor channel produced NO_2 with low translational energy and the propensity to absorb a second UV-photon and dissociate into NO and O [7]. Recent measurements, of infrared emission following photodissociation, by Wade *et al* [4] support the earlier suggestion by Lao *et al* [7] that, in this minor channel, NO is formed in its 2^2B_2 excited state.

Confusion remains in the details of the dissociation process via the lower energy $n \rightarrow \pi^*$ transition, though equation (1) does still appear to be the major channel [4]. Indeed the energetic threshold for equation (1) is 2.61 eV [6]. However in their recent measurements, Bernstein *et al* [9] appear to demonstrate that molecular dissociation via the $n \rightarrow \pi^*$ transition does *not* in fact occur, at least in a supersonic beam under collision-less conditions.

Other dissociative processes are also expected as minor channels [4], particularly via the $\pi \rightarrow \pi^*$ transition, including molecular elimination to form formaldehyde and HNO i.e.,

$$CH_3NO_2 + h\nu \rightarrow CH_2O + HNO. \quad (2)$$

The remarkable similarity between the HREELS results presented in figure 1 and earlier gas-phase data indicates that the electronic spectroscopy of condensed-phase NM, at least below ~8 eV, is essentially that of the gas phase. It is likely then, that dissociative processes occurring in condensed-phase

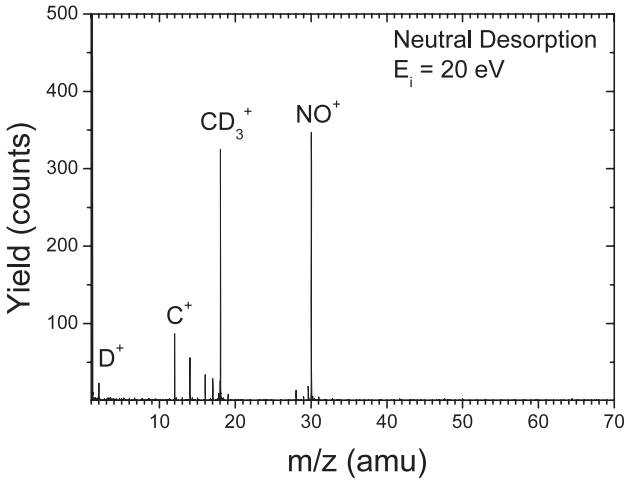

Figure 2. Mass spectrum of ions detected following non-resonant multi-photon ionization (NR-MPI) of neutral species desorbed by electron impact at 20 eV from a 4 monolayer (ML) thick film of CD_3NO_2 deposited on Pt at 35 K.

NM and d_3-NM will be similarly related to those previously observed in the gas phase and hence play a significant role in the electron stimulated desorption of neutral fragments from NM films.

4.2. ESD from nitromethane: detection of neutral fragments

The mass spectrum presented in figure 2 shows the positive ions detected following photo-ionization of the neutral species desorbed from a multilayer film of d_3-NM by 20 eV electrons. The mass spectrum is dominated by masses 18 and 30 amu, which measurements with non-deuterated nitromethane reveal as CD_3^+ and NO^+. Other fragments, notably D^+, C^+, CD^+ and CD_2^+ are also detected as well as a mass 17 (OH^+), which is likely due to sample contamination from H_2O in vacuum. The presence of the latter may suggest that signals at mass 16 and 18 also contain contributions from O^+ and H_2O^+. However preliminary measurements on the desorption of neutrals from water films [46], indicate that under similar conditions, the detected yield of O^+ is smaller (∼50%) than that of OH^+, while that of H_2O^+ is of only a slightly higher intensity, (∼130%). Therefore, the signals at mass 16 and 18 are primarily the result of electron interactions with d_3-NM. The signal at mass 29.5 corresponds to the detection of NO^+, formed directly by electron impact on the sample and injected into the ToF mass spectrometer before the passage of the photo-ionizing laser beam. Comparison with the mass spectra for cation desorption [16] suggests that directly desorbed cations represent less than 5% of the detected signals of CD_3^+ and NO^+ produced from neutral desorbing species at an incident electron energy of 20 eV. The minimum incident electron energies necessary for the desorption of CD_3^+ and NO^+ cations directly from multilayer d_3-NM were measured as 12.2 and 11.5 eV respectively, so that below incident energies of ∼12 eV, the signal detected in the present experiments derives entirely from the ionization of desorbed neutral species.

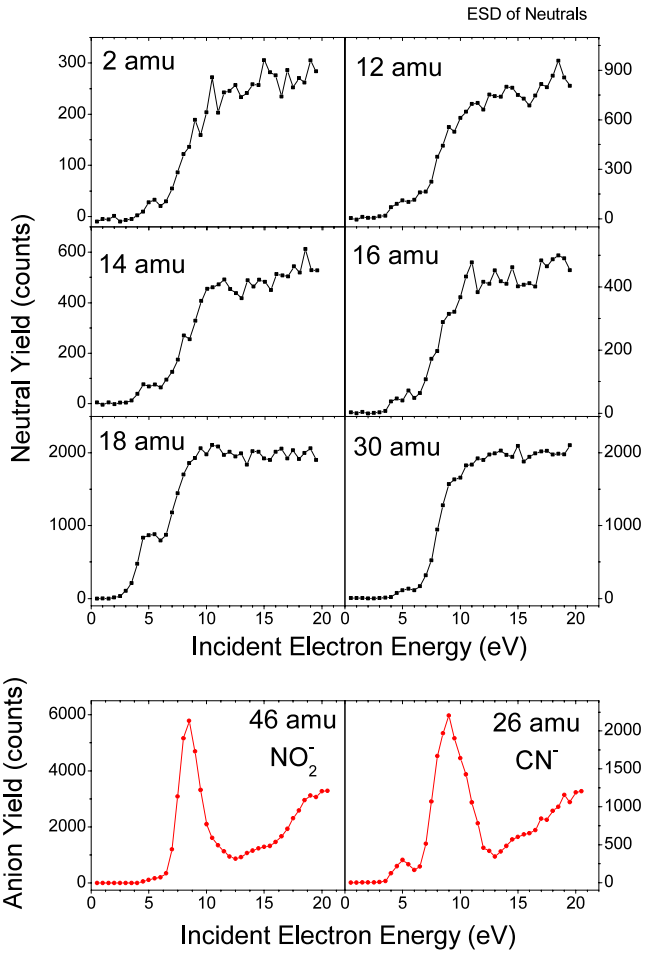

Figure 3. Yield functions of ions of mass 2, 12, 14, 16, 18, 30 amu, detected following NR-MPI of neutral species desorbed by electron impact on a 4 ML thick film of d_3-NM. Also shown in the lower panel are *anion* yield functions for CN^- and NO_2^- from [16].

Yield functions of each of the detected fragments are presented in figure 3. The yield functions of these neutral fragments are generally quite similar, with a low energy threshold (<3 eV) for a weak structure near 5 eV (most clearly seen for 18 amu, but present elsewhere) and then a sharp rise from ∼6 eV with a maximum near 10 eV. Above this energy the yields of the varying fragments remain constant or increase only slightly. The low energy structure (i.e., that seen below 6 eV) is particularly pronounced in the yield of CD_3 fragments, where the threshold appears to be less than 2.5 eV.

The energies of structures seen in the yield functions are thus similar to those previously identified with anion desorption via the DEA mechanism [16]. For comparison, anion yield functions for CN^- and NO_2^- are also shown in the lower panel of the figure. There appears a particularly strong correspondence between the low energy (∼3–6 eV) structure seen in the present data and a DEA resonance at the same energies, seen in the CN^- (most clearly) and NO_2^- yield functions. It is significant that the threshold energy for desorption in all cases is less than ∼3 eV, i.e., below the energy of the lowest electronic energy loss process (figure 1). In general, however, the overall form

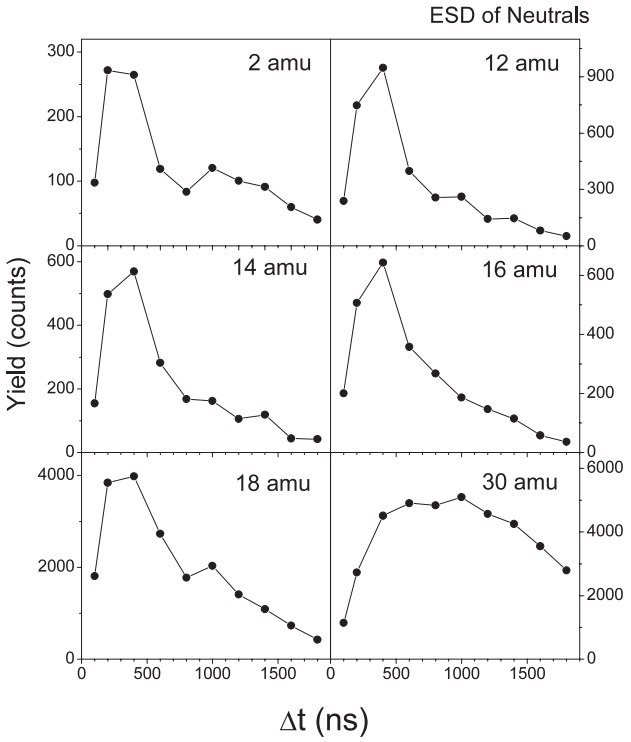

Figure 4. ESD yield at $E_i = 5$ eV of ions of mass 2, 12, 14, 16, 18, and 30 amu as a function of the time delay (Δt) between the incident electron pulse (of duration 50 ns) and that of the ionizing laser. Such *relative time of flight* distributions thus provide information on the energy distribution of neutral species particles desorbed from the film.

of the yield functions is somewhat reminiscent of those in the neutral desorption experiments of Feulner *et al* [32] on various low temperature molecular solids, for which it was suggested that non-dissociated neutral species were desorbed by a conversion of electronic to vibrational energy. Since non-resonant multi-photon ionization generates significant and complex fragmentation, it is not possible from the data of figures 2 and 3 alone to determine whether the detected neutral species are desorbed molecular fragments, resulting from LEE induced dissociation occurring within the solid, or fragments of d_3-NM desorbed intact from the film.

To obtain further information about the origin of neutral fragments, relative time of flight distributions were obtained by controlling the time delay Δt between the incident electron-pulse (duration 50 ns) and the passage of the ionizing laser shot. Figure 4 presents the ToF distribution data for electron impacts at 20 eV. Two important features are apparent in this figure. Firstly, the distributions appear highly structured suggesting that more than one desorption process is responsible for these signals. Secondly, many of the distributions are similar in form, in particular for fragments masses $\leqslant$18 amu, and this might be taken as evidence of their common formation via the laser induced dissociation of a larger moiety (i.e., a heavier fragment or even d_3-NM itself). However there are significant differences between the distributions measured for the two strongest signals (NO^+ and CD_3^+) which indicate that in at least one of these two cases, desorption of the original neutral fragment proceeds via a dissociative process.

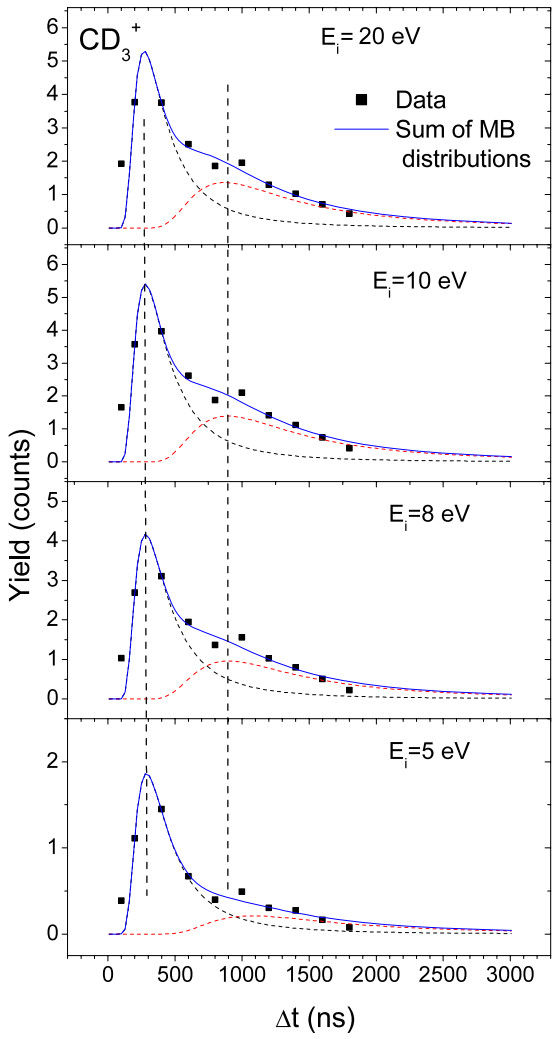

Figure 5. Relative time of flight distributions for detected ions of mass 18 amu as measured at 5, 8, 10 and 20 eV. The experimental data can be well fitted using a minimum of *two* modified Maxwell–Boltzmann distributions [47]. See the text for details of the fitting procedure and table 1 for the characteristic temperature of each distribution.

In figure 5 we illustrate in greater detail, relative ToF distributions obtained for the CD_3 fragment at incident electron energies of 5, 8, 10 and 20 eV. As in the work of Petrik *et al* [47], we have attempted to fit these relative ToF curves as the sum of modified Maxwell–Boltzmann type distribution functions having the form,

$$Y(t) = \sum_i C_i t^{-3} \exp\left(-\frac{m}{2kT_i}\frac{d^2}{\Delta t^2}\right) \qquad (3)$$

where $Y(t)$ is the neutral yield, C_i is a proportionality constant for the ith Maxwell–Boltzmann distribution, m is the mass of the neutral desorbate, k is Boltzmann's constant, d is the flight distance from the sample surface to the probe laser beam (taken as 0.5 mm), Δt is the time delay between the electron and laser beam pulses and T_i is the effective temperature of the ith distribution. Curve fitting was performed using the Levenberg–Marquardt algorithm as implemented within the MathCad software package.

Table 1. Representative temperatures and their standard error, determined for Maxwell–Boltzmann distributions fitted to the yields of neutral fragment CD_3, averages over 5–20 eV incident electron energy.

	Assuming $m = 18$ amu	Assuming $m = 64$ amu
T_1	2339 ± 20 K	8317 ± 1848 K
T_2	210 ± 7 K	746 ± 24 K

It is clear from figure 5, that at all incident electron energies, the measured ToF data are well fitted by only two Maxwell–Boltzmann distributions of hyper-thermal energy. However, it is unclear whether the detected CD_3^+ signal derives from the direct desorption of a CD_3 neutral fragments from the film or from photo-ionization of a desorbed d_3-NM molecule. We have thus calculated the effective temperatures of the Maxwell–Boltzmann distributions assuming both cases (i.e., desorption as mass 18 and as mass 64) and show these results in table 1. The uncertainties given in the table reflect the statistical variation observed between effective temperatures obtained at different incident energies. However, it should be noted that the absolute values of the effective temperature are, via equation (3), dependant on distance d^2, so that a small relative error in d would lead to much larger (by factor 2) error in the temperature. The relative ToF distributions for CD_3 are dominated by a prompt peak, the position of which is invariant with incident electron energy. A second, slower distribution is also observed. The contribution of this second distribution is relatively weak in the data obtained at incident electron energies <8 eV and there is some evidence that this distribution also moves to marginally higher temperature above this energy. Above the 8 eV threshold, the relative ToF distributions are remarkably similar, apart from their overall intensities.

A similar fitting procedure was attempted for the detected fragment of mass 30 (NO^+), and examples of these fits and relative ToF distributions are presented in figure 6 for several incident electron energies. As before, due to our uncertainty in the mass of the desorbed neutral species we present, in table 2, characteristic temperatures for each of the fitted Maxwell–Boltzmann distributions, assuming that the desorbed neutral has either mass 30 (NO), 46 (NO_2, see below) or 64 amu (d_3-NM). As can be seen from the figure (and table), at least three hyper-thermal MB distributions are needed to adequately fit the ToF data. In fact, there are probably not sufficient experimental data points to warrant inclusion of the fastest peak, yet we were unable to fit the data with only two modified Maxwell–Boltzmann distributions. This could of course indicate that at least one of the desorbed particle energy distributions is poorly represented by a modified MB distribution. Once more we note that the absolute values of effective temperatures given in the table are highly sensitive to the distance between the sample and the laser probe.

As noted earlier, the dissimilarity between the relative ToF distributions for the detected CD_3^+ and NO^+ signals indicates that molecular dissociation must occur in the film following electron impact. Not only are the behaviors at the shortest Δt quite different, but the dissimilarity continues across the entire relative ToF distribution. This is borne out in the data of tables 1 and 2, where it is important to note that, when an intact NM molecule (mass 64) is assumed to be the original desorbed neutral species, there is no correspondence between the temperatures of the Maxwell–Boltzmann distributions observed for the two fragments. *This is a strong indication that the desorption of intact* d_3*-NM molecules and their photon-*

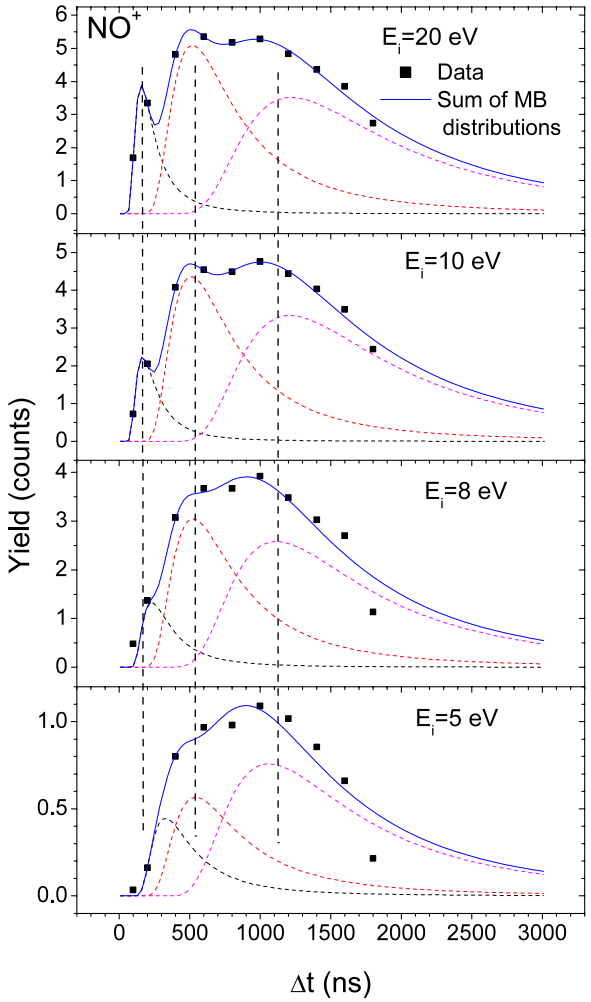

Figure 6. Relative time of flight distributions for detected ions of mass 30 amu as measured at 5, 8, 10 and 20 eV. The experimental data can be well fitted using a minimum of *three* modified Maxwell–Boltzmann distributions [47]. See the text for details of the fitting procedure and table 2 for the characteristic temperature of each distribution.

Table 2. Representative temperatures (and their standard error) determined for Maxwell–Boltzmann distributions fitted to the yields of neutral fragment NO, averages over 5–20 eV incident electron energy.

	Assuming $m = 30$ amu	Assuming $m = 46$ amu	Assuming $m = 64$ amu
T_1	$11\,100 \pm 194$ *K*	$17\,020 \pm 198$ *K*	$23\,670 \pm 415$ *K*
T_2	1239 ± 25 K	1900 ± 39 *K*	2644 ± 54 *K*
T_3	243 ± 9 K	372 ± 14 *K*	518 ± 20 *K*

induced dissociation is not an important contributor to the observed yields of both CD_3^+ *and* NO^+. Moreover, the almost complete invariance with incident electron energy of the relative ToF distributions seen in figures 5 and 6 is significant, as it indicates that the same dissociation process (or processes) operate across the entire range of incident electron energy.

Bearing these points in mind, and considering NO^+ the primary product of the non-resonant photo-ionization of NO_2 [48], we propose that the strong neutral desorption signal of CD_3 and NO derives from the dissociation of CD_3NO_2 into CD_3 and NO_2 which photolysis studies [4–9] indicate proceeds via excitation of NM's lowest two electronic bands. Consequently, the neutral desorption signal from about 3 eV and the sharp rise in neutral signal seen at about 6 eV might quite plausibly be associated with firstly, the onset for excitation of the weak n or $\sigma \rightarrow \pi^*$ transition(s), and subsequently the onset the strong $\pi \rightarrow \pi^*$. As noted earlier, at least two different pathways to the production of NO_2 and CH_3 (CD_3) exist via excitation of the $^1B_2$ state and these are distinguished both by the final state of the NO_2 fragment ($\tilde{A}^2B_2$ or 2^2B_2) and the kinetic energy imparted to the fragments. It is thus to be expected that the relative ToF measurements for CD_3 (figure 5) should show two hyper-thermal distributions. Similarly, the fact that NO can form both by the photo-ionization of a desorbed NO_2 fragment and spontaneously by the decay of excited NO_2 ($\tilde{A}^2B_2$) may explain the complicated ToF data presented in figure 6.

The invariance of the ToF data presented in figures 5 and 6 for incident electron energies greater than 7 eV, further indicates that, similar to the suggestion made by Rakhovskaia *et al* [32] when describing neutral desorption from other molecular solids, there must exist efficient mechanisms to quench higher electronic excitations and return excited molecules to the lowest $\pi \rightarrow \pi^*$ transition.

We expect the other neutral fragments to be photo-fragments of the desorbed neutrals. Fragments such as D^+, C^+, CD^+ and CD_2^+ are expected to be produced via non-resonant photo-ionization of CD_3 [48] (an addition to that of d_3-NM), so that the general similarities observed in the relative ToF data for these masses presented in figure 4 appears reasonable, while O^+ might be expected from the photodissociation of NO and NO_2.

Excitation of the $^1B_2$ state or the lower-lying n or $\sigma \rightarrow \pi^*$ transition can not however explain the very low energy thresholds for neutral particle desorption i.e., at energies <3 eV, below the threshold for excitation of the lowest energy loss manifold (figure 1). Under these circumstances only the mechanism of DEA can account for the desorbed signal. The low energy desorption signal is most noticeable for the CD_3 fragment, while in the gas phase, the strongest anion signal from NM is its conjugate, NO_2^- [47, 48]. It is likely then, that in the present experiments, at energies >3 eV, we are observing CD_3 generated by the reaction,

$$CD_3NO_2 + e^- \rightarrow (CD_3NO_2)^- \rightarrow CD_3 + NO_2^-. \quad (4)$$

This process is observed to have a maximum cross section near 0.7 eV in gas-phase experiments [47, 48]. It is likely that the apparent threshold energy for desorption of CH_3 in figure 3 may reflect both the poor performance of the present electron gun at energies below ∼2 eV and the difficulty of detecting desorbed fragments of very low KE.

It is also likely that the structure seen in the yield functions of the various ions detected following photo-ionization, (figure 3) contains contributions of neutrals desorbed following DEA to NM via higher-lying resonances (i.e., those observed at 9–10 eV and ∼14 eV in the anion yield functions [16]). It is also possible, however, that these structures, while associated with TNI, are not the result of DEA but rather of resonant excitation of other neutral electronic states that subsequently decay into a neutral dissociative channel.

Of course some loose ends remain. For example, it is unlikely that excitation of the lowest electronic band of NM (n or $\sigma \rightarrow \pi^*$ transition) could produce NO_2 (and hence NO) by the same pathways as the higher band. Yet the relative ToF data below $E_I = 5.5$ eV are only subtly different from that measured above the threshold of the $\pi \rightarrow \pi^*$ band. This latter result would seem to indicate that, contrary to recent photolysis measurements [9], dissociation via electron impact at incident energies commensurate with excitation of the lower band is indeed possible for condensed NM.

5. Conclusion

Nitromethane has long been considered a simple molecular prototype for explosive materials, yet the dissociative molecular processes thought responsible for the rapid propagation of exothermic chemical reactions through condensed NM have rarely been studied in other than the gas phase. In these experiments, we observe for solid NM, that the same molecular dissociation processes studied in the gas phase, appear to be responsible for the desorption of various molecular fragment species into vacuum. While the absolute yields of these fragments are dependent on the energy of the exciting radiation (here low energy electrons) and increase with increasing incident energy, our tentative measurements of fragment kinetic energy show little variation. It seems likely that at energies >∼5 eV, molecular dissociation proceeds via the low-lying dissociative states such as the $^1B_1$ and $^1B_2$ states and that higher-lying states couple to these end points.

Nevertheless at energies below that necessary for excitation of dissociative electronic states, we also observe the desorption of neutral fragments. Dissociative electron attachment is the only plausible explanation for this signal and is supported by our previous measurements of anion desorption from similarly prepared deuterated nitromethane films [16].

Acknowledgments

This paper is dedicated to the memory of our colleague and friend, Professor Theodore E Madey. This work is financed by the Canadian Institutes of Health Research (CIHR) and by the Natural Sciences and Engineering Research Council of Canada. SP gratefully acknowledges financial support from CIHR in the form of a Postdoctoral Fellowship.

References

[1] Borrmann A and Martens C G 1995 *J. Chem. Phys.* **102** 788
[2] Hervout A, Desbiens N, Bourasseau E and Maillet J-B 2002 *J. Phys. Chem.* B **112** 5070
[3] Reed E J, Riad Manaa M, Fried L E and Glaesemann K R 2008 *Nat. Phys.* **4** 72
[4] Wade E A, Reak K E, Li S L, Clegg S M, Zou P and Osborn D L 2006 *J. Phys. Chem.* A **110** 4405–12
[5] Blais N C 1983 *J. Chem. Phys.* **79** 1723
[6] Butler L J, Krajnovich D, Lee Y T, Ondrey G and Bersohn R 1983 *J. Chem. Phys.* **79** 1708
[7] Lao K Q, Jensen E, Kash P W and Butler L J 1990 *J. Chem. Phys.* **93** 3958
[8] Moss D B, Trentelman K A and Houston P L 1992 *J. Chem. Phys.* **96** 237
[9] Guo Y Q, Bhattacharya A and Bernstein E R 2009 *J. Phys. Chem.* A **113** 85
[10] Tsuda S, Yokohata A, Kawai M and Bullet M 1969 *Chem. Soc. Japan* **42** 607–14
Tsuda S, Yokohata A, Kawai M and Bullet M 1969 *Chem. Soc. Japan* **42** 614–8
Tsuda S, Yokohata A, Kawai M and Bullet M 1969 *Chem. Soc. Japan* **42** 1515–8
[11] di Domenico A and Franklin J L 1972 *Int. J. Mass Spectrom. Ion Phys.* **9** 171
[12] Walker I C and Fluendy M A D 2001 *Int. J. Mass Spectrosc.* **205** 171–82
[13] Sailer W, Pelc A, Matejcik S, Illenberger E, Scheier P and Märk T D 2002 *J. Chem. Phys.* **117** 7989
[14] Alizadeh E, Ferreira da Silva F, Zappa F, Mauracher A, Probst M, Denifl S, Bacher A, Märk T D, Limão-Vieira P and Scheier P 2008 *Int. J. Mass Spectrom.* **271** 15–21
[15] Blais N C, Engelke R and Sheffield S A 1997 *J. Phys. Chem.* A **101** 8285
[16] Bazin M, Ptasinska S, Bass A D and Sanche L 2009 *Phys. Chem. Chem. Phys.* **11** 1610
[17] Bass A D and Sanche L 2004 *Charge Particle and Photon Interactions with Matter: Chemical, Physiochemical and Biological Consequences with Applications* ed Y Hatano and A Mozumder (New York: Dekker)
[18] Feulner P and Menzel D 1995 *Laser Spectrocopy and Photochemistry on Metal Surfaces* ed H-L Dai and W Ho (Singapore: World Scientific) chapter 16
[19] Huels M A, Parenteau L, Cloutier P and Sanche L 1995 *J. Chem. Phys.* **103** 6775–82
[20] Bass A D, Lezius M, Ayotte P, Parenteau L, Cloutier P and Sanche L 1997 *J. Phys. B: At. Mol. Phys.* **30** 3527–41
[21] Lane C D and Orlando T M 2006 *J. Chem. Phys.* **124** 164702
[22] Kimmel G A, Orlando T M, Vezina C and Sanche L 1994 *J. Chem. Phys.* **101** 3282–6
Kimmel G A, Orlando T M, Cloutier P and Sanche L 1997 *J. Phys. Chem.* B **101** 6301–3
Kimmel G A and Orlando T M 1996 *Phys. Rev. Lett.* **77** 3983–6
[23] Dugal P-C, Huels M A and Sanche L 1999 *Radiat. Res.* **151** 325
[24] Dugal P-C, Abdoul-Carime H and Sanche L 2000 *J. Phys. Chem.* B **104** 5610
[25] Menzel D and Gomer R 1964 *J. Chem. Phys.* **40** 1164
Menzel D and Gomer R 1964 *J. Chem. Phys.* **41** 3311
[26] Redhead P A 1964 *Can. J. Phys.* **42** 886
[27] Antoniewicz P R 1980 *Phys. Rev.* B **21** 3811
[28] Zimmerer G 1994 *Nucl. Instrum. Methods* B **91** 601
[29] Coletti F, Debever J M and Zimmerer G 1984 *J. Phys. Lett.* **45** L467
[30] Shi H, Cloutier P and Sanche L 1995 *Phys. Rev.* B **52** 5385–91
[31] Cui S T, Cummings P T and Johnson R E 1989 *Surf. Sci.* **222** 491
[32] Rakhovskaia O, Wiethoff P and Feulner P 1995 *Nucl. Instrum. Methods Phys. Res.* B **101** 169–73
[33] Ibach H 1991 *Electron Energy Loss Spectrometers* (Berlin: Springer)
[34] Swiderek P, Schürfeld S and Winterling H 1997 *Ber. Bunsenges. Phys. Chem.* **101** 1517
[35] Winterling H, Haberkern H and Swiderek P 2001 *Phys. Chem. Chem. Phys.* **3** 4592
[36] Göötz B, Winterling H and Swiderek P 1999 *J. Electron Spectrosc.* **105** 1
[37] Reimann C T, Brown W L, Nowakowski M J, Cui S T and Johnson R E 1990 *Desorption Induced by Electronic Transistions DIET IV* ed G Betz and P Varga (Berlin: Springer) p 226
[38] Leclerc G, Bass A D, Mann A and Sanche L *Phys. Rev.* B **46** 4865
[39] Dehmer P M, Dehmer J L and Pratt S T 1987 *Comments At. Mol. Phys.* **19** 205
[40] See, for example, Hasselbrink E 1995 *Laser Spectrocopy and Photochemistry on Metal Surfaces* ed H-L Dai and W Ho (Singapore: World Scientific) chapter 17
[41] Lockyer N P and Vickerman J C 1997 *Laser Chem.* **17** 139
[42] Gedanken A, Robin M B and Kuebler N A 1982 *J. Phys. Chem.* **86** 4096
[43] Yang J J, Gobeli D A and El-Sayed M A 1985 *J. Phys. Chem.* **89** 3426
[44] Lockyer N P and Vickerman J C 1998 *Int. J. Mass Spectrom.* **176** 77–86
[45] Flicker W M, Mosher O A and Kuppermann A 1979 *Chem. Phys. Lett.* **60** 518 and references therein
[46] Bazin M, Bass A D and Sanche L, unpublished
[47] Petrik N G, Knutsen K, Paparazzo E, Lea S, Camaioni D M and Orlando T M 2000 *J. Phys. Chem.* B **104** 1563–71
[48] Kilic H S, Ledingham K W D, Kosmidis C, McCanny T, Singhal R P, Wang S L, Smith D J, Langley A J and Shaikh W 1997 *J. Phys. Chem.* A **101** 817–23